M

Morphologically Detailed Cellular and Pool Motoneuron Models

Sherif M. Elbasiouny[1,2] and Mohamed H. Mousa[2]
[1]Department of Neuroscience, Cell Biology, and Physiology, Wright State University, Dayton, OH, USA
[2]Department of Biomedical, Industrial and Human Factors Engineering, Wright State University, Dayton, OH, USA

Definition

Morphologically detailed motoneuron models refer to a class of motoneuron (MN) models that are developed using experimentally derived, three-dimensional digital reconstructions of MN morphology (Fig. 1, left panel). In contrast to models with reduced morphological detail (Fig. 1, right panel), these models offer more accurate spatial resolution and allow realistic distribution of electrical properties.

Detailed Description

In a computer simulation, each part of the membrane is represented by an isopotential (i.e., fixed potential) compartment governed by a system of differential equations (see "▶ Compartmental Models of Spinal Motoneurons"). These equations calculate the membrane electrical properties and ion channel behaviors/kinetics. Therefore, in order to have accurate spatial resolution, each compartment should be very small in length ($<0.1\lambda$, λ is the space constant) (Fleshman et al. 1988; Clements and Redman 1989). Because of the intricacy of a MN's structure, a morphologically detailed computer model would typically have thousands of compartments to fully represent the MN. Simplified computer models (also known as "equivalent cable models" or "reduced models"), on the other hand, represent the dendritic morphology with a single unbranched cable which contains membrane surface area equivalent to all real dendrites combined – thus "equivalent cable." This cable usually comprises 10–50 compartments (but might sometimes only contain one).

Development of Computer Models with Realistic Morphology

The first step in constructing a morphologically detailed computer model is importing the three-dimensional morphology of the cell, which is usually obtained from the reconstruction of intracellularly stained or retrograde-labeled MNs. Examples of reconstructed morphologies are available through the online database NeuroMorpho.Org (http://neuromorpho.org/neuroMorpho/index.jsp). The second step in model development is matching the passive electrical properties of the model cell to

D. Jaeger, R. Jung (eds.), *Encyclopedia of Computational Neuroscience*,
https://doi.org/10.1007/978-1-4614-7320-6_371-2

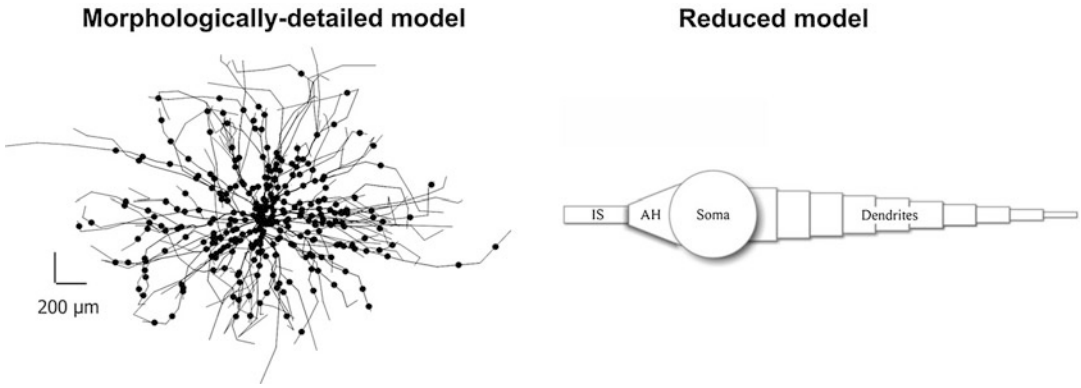

Morphologically Detailed Cellular and Pool Motoneuron Models, Fig. 1 A morphologically detailed model (left) versus its reduced counterpart for the same MN [cell 43c5, originally published in Cullheim et al. 1987]

experimental data. This step involves setting the passive membrane parameters [e.g., specific transmembrane resistance (R_m), specific axial membrane resistance (R_a), and specific membrane capacitance (C_m)] of each compartment of the model cell to replicate those electrical properties in which active conductances have little or no contribution (e.g., MN input resistance, time constants, electrotonic length). The third step is matching the active electrical properties of the model cell to experimental data. This is the point at which decisions are made on what active conductances need to be included and what their spatial distributions on various cell structures should be (soma, initial segment, and dendrites). The ionic current, I_{ion}, mediated through each active conductance can be described by the following general expression:

$$I_{\text{ion}} = g_{\text{ion}} \times (V_m - E_{\text{ion}}) \quad (1)$$

$$g_{\text{ion}} = \overline{g}_{\text{ion}} \times m^n \times h^l \quad (2)$$

in which g_{ion} is the varying conductance of the ion channel; $\overline{g}_{\text{ion}}$ is the maximum conductance of the ion channel; m and h are the activation and inactivation state variables, respectively; and n and l are the order of activation and inactivation, respectively.

For each membrane state variable (η), the time and voltage dependence are given by

$$d\eta/dt = \alpha_\eta(1-\eta) - \beta_\eta\eta \quad (3)$$

$$\tau_\eta = 1/(\alpha_\eta + \beta_\eta) \quad (4)$$

The spatial distribution, densities ($\overline{g}_{ion}$), and activation and inactivation kinetics (α_η, β_η, τ_η) of individual active conductances are then adjusted to produce comparable firing behaviors to experimental data (see "▶ Compartmental Models of Spinal Motoneurons," for examples on how calcium channels are distributed in order to replicate plateau potentials successfully). A computer model would be validated if it matches multiple sets of experimental data (passive and active) under various experimental conditions (current clamp and voltage clamp). To test the robustness and validity of model results, sensitivity analysis is usually required on critical model parameters. In this process, model parameters that greatly impact the simulation results are first identified. Then, their values are varied within the range observed in experimental recordings in order to assess the dependence of output model behaviors on the variation in those parameters.

Utility of Morphologically Detailed MN Models

Simplified MN models were developed as a necessary means to make simulations computationally efficient, an issue which is being resolved by

increasing computational power. Morphologically detailed computer models are now more feasible and offer numerous attractive features. First, they can be used to investigate both the passive and active properties of MNs. In contrast, the dendritic reduction of reduced models is unable to accurately reproduce active conditions (Rall 1962; Holmes et al. 1992). Second, the incorporation of full MN morphology allows these detailed models to simulate MN firing behaviors more accurately, whereas reduced models are unable to simulate some MN firing behaviors (Jackson and Cauller 1997; Hendrickson et al. 2011). This is because the equivalent membrane surface area, even when optimized to match a real MN's electrical properties, is not the only factor which affects active conductances: The morphology of dendrites – the number of branches and the direction of branching – also affects dendritic active conductances. Third, morphologically detailed models contain enough anatomical data to produce unique solutions to questions about passive properties – that is, a single scenario or a single set of model parameters can account for all aspects of empirical data (Holmes and Rall 1992; Holmes et al. 1992). This is in contrast to reduced models, which suffer great *redundancy* of model parameters – that is, they produce too many potential solutions to a question or too many candidate mechanisms to feasibly test in experiments (Holmes and Rall 1992; Holmes et al. 1992). Fourth, morphologically detailed models allow investigation of scientific questions impacted by the specific spatial distribution of various cellular properties (e.g., spatial distribution of dendritic ion channels and synaptic inputs), which are not faithfully represented in reduced models (Elbasiouny et al. 2005). Finally, in neurological conditions, such as spinal cord injury or amyotrophic lateral sclerosis, the MN experiences massive pathological changes in dendritic morphology (Kitzman 2005; Amendola and Durand 2008). Because accurate modeling of changes in dendritic structure is critical for accurate simulation of these pathologies, morphologically detailed models would be more appropriate to use in such neurological conditions, as opposed to reduced models which lack dendritic morphological detail.

Simulations of Pool Models Formed from Morphologically Detailed MN Models

Although morphologically detailed cell models are useful for studying MN behaviors at the cellular level, muscle and network behaviors require highly detailed pool models in which a number of MNs are included to represent the pool of spinal neurons innervating the muscle of interest (Jiang et al. 2015; Allen and Elbasiouny 2018). These pool models (Fig. 2) could then be used to examine the neuronal drive to the muscle, the recruitment pattern of MNs, and the total as well as individual forces and EMG signals generated by the different fiber types comprising the muscle. For example, Fig. 2 shows an example of a motor pool from Allen and Elbasiouny (2018): 51 morphologically detailed cells were incorporated into a pool model in order to simulate the motor nerve's neural activity, as well as the resulting compound action potentials, muscle EMG, and force from individual MN spikes. With such a pool, muscle and individual motor unit behaviors could be examined under different conditions and in response to different synaptic inputs.

Despite the advantages of 3D morphologically detailed pool models, there are challenges in their operation and development. Operation of a pool model formed of morphologically detailed cells requires high computational power and involves long run times. Computational resources such as parallel supercomputer hardware [e.g., the Neuroscience Gateway (Sivagnanam et al. 2013)] are therefore critical for such simulations. In these simulations, the run time is determined by the complexity of individual model cells, the architecture of the pool model, and how cells communicate with each other. Accordingly, the run time will be governed by the slowest and most complex cell in the pool model.

Challenges in the development of pool models include consideration of several key design choices. Importantly, several design considerations were shown to have a strong impact on

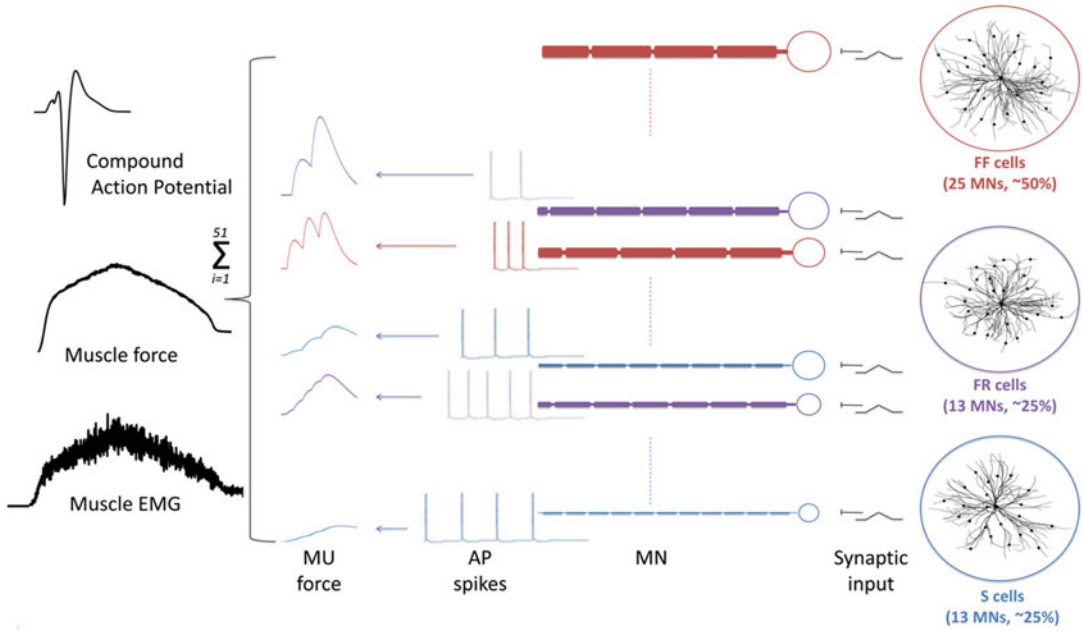

Morphologically Detailed Cellular and Pool Motoneuron Models, Fig. 2 Example of a MN pool model, from right to left: a morphologically detailed MN model is activated by triangular synaptic commands. Somatic action potentials are generated; these can then be used to calculate the force and EMG signals of each motor unit and the compound action potential, total force, and EMG from the whole pool. (Adapted from Allen and Elbasiouny (2018) with permission)

simulation predictions made by morphologically detailed MN pool models (Allen and Elbasiouny 2018). The features tested included (1) the number of model cells to include in the pool; (2) whether MN types were explicitly represented (slow-twitch vs. fatigue-resistant vs. fast-twitch); (3) whether MN types were modeled using generic templates versus those developed with distinct electrical and morphological properties; (4) whether different MN types were modeled with overlapping cellular properties or with discrete property ranges; (5) whether biological heterogeneity in cellular properties within MN types was simulated; and (6) whether comprehensive experimental data were available for model verification. Specifically, MN recruitment pattern, firing rates, and force data were shown to be affected by these design choices. Figure 3 illustrates four examples of possible design choices for the pool model. Figure 3a shows a pool model with overlap in the properties of the different MN types. Figure 3b shows a pool model with discrete ranges (i.e., no overlap) in the properties of MN types. In Fig. 3a, b, MN types were modeled using discrete templates. Figure 3c, on the other hand, shows a pool model in which MN types were represented by generic templates and without overlap in properties. Finally, Fig. 3d shows a pool model which simulates biological heterogeneity in individual MNs within each type. As shown in panels e–h, the recruitment pattern of MNs was affected significantly by these design choices. In various scenarios, mixed or reverse recruitment patterns could be suppressed or exaggerated. In sum, incorporating high levels of detail into pool simulations requires careful consideration of the scientific question being investigated and of the cost vs. benefit of each feature, in order to choose the most relevant pool model design features. However, the effort is justified by the high fidelity of these simulations to the observed experimental data.

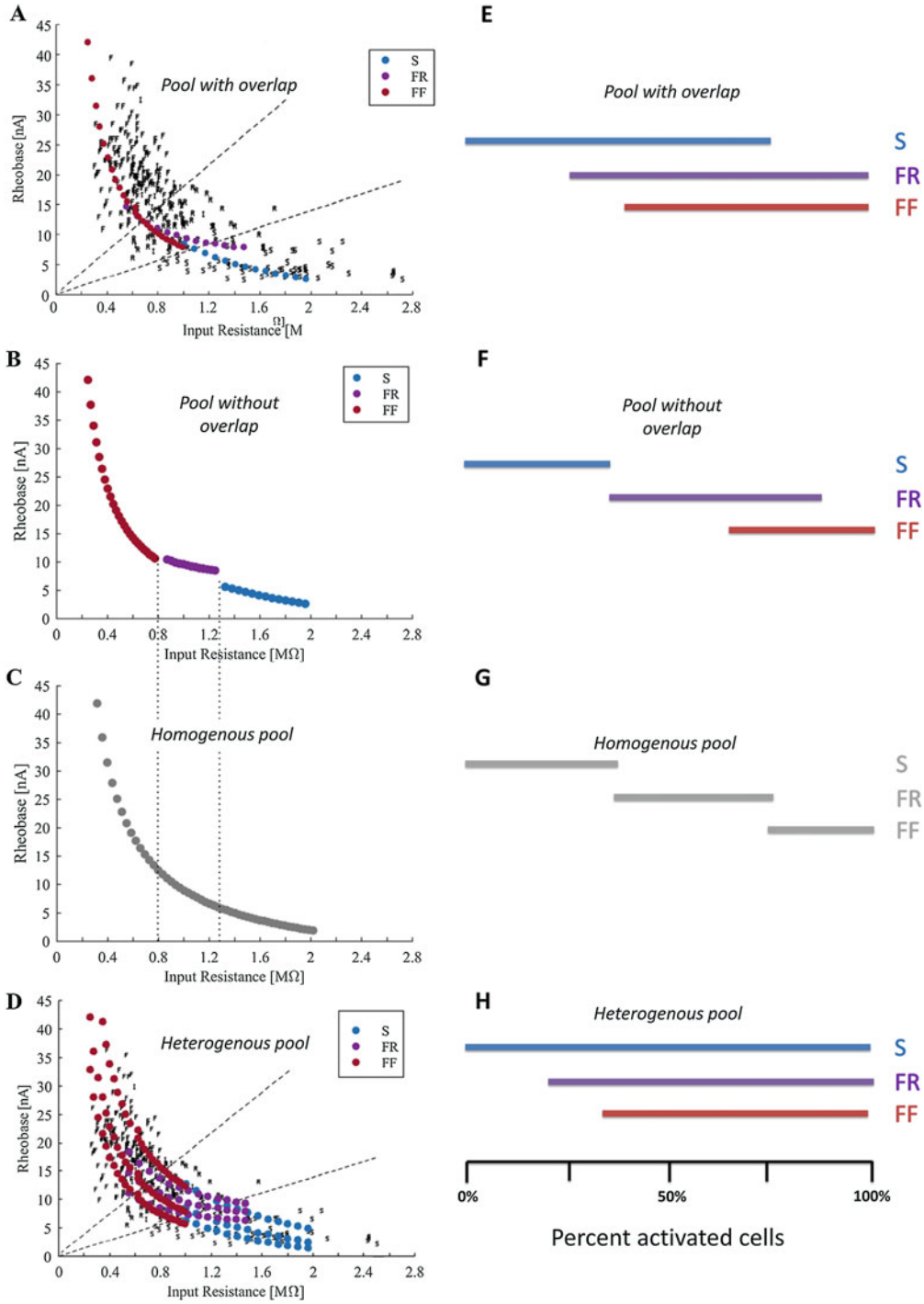

Morphologically Detailed Cellular and Pool Motoneuron Models, Fig. 3 Rheobase versus input resistance for pool models of different design features. (**a**) Pool model with overlap in MN-type cellular properties. (**b**) Pool model with discrete ranges of MN-type properties (i.e., no overlap). (**c**) Homogenous pool model in which MN types are modeled using generic cell templates with varied electrical properties. (**d**) Pool model which simulates heterogeneity in individual MN properties within MN types. (**e**, **f**) The recruitment range of MN types in each pool model. (Adapted from Allen and Elbasiouny (2018) with permission)

Cross-References

► Compartmental Models of Spinal Motoneurons

Acknowledgements Funding for this work was provided to SE by (1) the US National Institute of Health-National Institute of Neurological Disorders and Stroke (NIH-NINDS) grant #NS091836 and (2) the National Academy of Sciences (NAS) and the US Agency for International Development (USAID) NAS Subaward No. 2000009148. Any opinions, findings, conclusions, or recommendations expressed in this entry are those of the authors alone and do not necessarily reflect the views of USAID or NAS.

References

Allen JM, Elbasiouny SM (2018) The effects of model composition design choices on high-fidelity simulations of motoneuron recruitment and firing behaviors. J Neural Eng 15:036024

Amendola J, Durand J (2008) Morphological differences between wild-type and transgenic superoxide dismutase 1 lumbar motoneurons in postnatal mice. J Comp Neurol 511:329–341

Clements JD, Redman SJ (1989) Cable properties of cat spinal motoneurones measured by combining voltage clamp, current clamp and intracellular staining. J Physiol 409:63–87

Cullheim S, Fleshman JW, Glenn LL, Burke RE (1987) Membrane area and dendritic structure in type-identified triceps surae alpha motoneurons. J Comp Neurol 255:68–81

Elbasiouny SM, Bennett DJ, Mushahwar VK (2005) Simulation of dendritic Cav1.3 channels in cat lumbar motoneurons: spatial distribution. J Neurophysiol 94:3961–3974

Fleshman J, Segev I, Burke R (1988) Electrotonic architecture of type-identified alpha-motoneurons in the cat spinal cord. J Neurophysiol 60:60–85

Hendrickson EB, Edgerton JR, Jaeger D (2011) The capabilities and limitations of conductance-based compartmental neuron models with reduced branched or unbranched morphologies and active dendrites. J Comput Neurosci 30:301–321

Holmes WR, Rall W (1992) Estimating the electrotonic structure of neurons with compartmental models. J Neurophysiol 68:1438–1452

Holmes WR, Segev I, Rall W (1992) Interpretation of time constant and electrotonic length estimates in multicylinder or branched neuronal structures. J Neurophysiol 68:1401–1420

Jackson ME, Cauller LJ (1997) Evaluation of simplified compartmental models of reconstructed neocortical neurons for use in large-scale simulations of biological neural networks. Brain Res Bull 44:7–17

Jiang MC, Elbasiouny SM, Collins WF 3rd, Heckman CJ (2015) The transformation of synaptic to system plasticity in motor output from the sacral cord of the adult mouse. J Neurophysiol 114:1987–2004

Kitzman P (2005) Alteration in axial motoneuronal morphology in the spinal cord injured spastic rat. Exp Neurol 192:100–108

Rall W (1962) Theory of physiological properties of dendrites. Ann N Y Acad Sci 96:1071–1092

Sivagnanam S, Majumdar A, Yoshimoto K, Astakhov V, Bandrowski A, Martone ME, Carnevale NT (2013) Introducing the Neuroscience Gateway. IWSG 993